Coustenis, A., Bampasidis, G., Achterberg, R. K., Lavvas, P., Jennings, D. E., Nixon, C. A., ... Stamogiorgos, S. (2013). EVOLUTION OF THE STRATOSPHERIC TEMPERATURE AND CHEMICAL COMPOSITION OVER ONE TITANIAN YEAR. Astrophysical journal, 779(2), [177]. 10.1088/0004-637X/779/2/177

The Astrophysical Journal, 779:177 (9pp), 2013 December 20 doi:10.1088/0004-637X/779/2/177

EVOLUTION OF THE STRATOSPHERIC TEMPERATURE AND CHEMICAL COMPOSITION OVER ONE TITANIAN YEAR

Athena Coustenis[1], G. Bampasidis[1,2], R. K. Achterberg[3,4], P. Lavvas[5], D. E. Jennings[3], C. A. Nixon[3], N. A. Teanby[6], S. Vinatier[1], F. M. Flasar[3], R. C. Carlson[3,7], G. Orton[8], P. N. Romani[3], E. A. Guandique[3,9], and S. Stamogiorgos[2,10]
[1] Laboratoire d'Etudes Spatiales et d'Instrumentation en Astrophysique (LESIA), Observatoire de Paris, CNRS, UPMC Univ. Paris 06, Univ. Paris-Diderot, 5, place Jules Janssen, F-92195 Meudon Cedex, France; athena.coustenis@obspm.fr
[2] Faculty of Physics, National and Kapodistrian University of Athens, Panepistimioupolis, GR 15783 Zographos, Athens, Greece
[3] NASA/Goddard Space Flight Center, Greenbelt, MD 20771, USA
[4] Department of Astronomy, Stadium Drive, University of Maryland, College Park, MD 20742-2421, USA
[5] GSMA, Université Reims Champagne-Ardenne, F-51687 Reims Cedex 2, France
[6] School of Earth Sciences, University of Bristol, Bristol BS8 1RJ, UK
[7] IACS, Catholic University of America, Washington, DC 20064, USA
[8] MS 183-501, Jet Propulsion Laboratory, California Institute of Technology, 4800 Oak Grove Drive, Pasadena, CA 91109, USA
[9] Adnet Systems, Inc., Rockville, MD 20852, USA
[10] Technische Universität München (TUM), D-80333 Munich, Germany
Received 2013 September 4; accepted 2013 October 23; published 2013 December 4

ABSTRACT

Since the *Voyager 1* (*V1*) flyby in 1980, Titan's exploration from space and the ground has been ongoing for more than a full revolution of Saturn around the Sun (one Titanian year or 29.5 Earth years had elapsed in 2010 May). In this study, we search for temporal variations affecting Titan's atmospheric thermal and chemical structure within that year. We process *Cassini*/CIRS data taken during the Titan flybys from 2006–2013 and find a rather uneventful equatorial evolution. Conversely, at northern latitudes, we found enhanced abundances around the period of the northern spring equinox in mid-2009, which subsequently decreased (from 2010 to 2012), returning to values similar to those found in the *V1* epoch, one Titanian year before. In the southern latitudes, since 2012, we see a trend for an increase of several trace gases (C_4H_2, C_3H_4, and HCN), indicative of a seasonal atmospheric reversal setting in. When we compare the CIRS 2010 and the 1980 *V1*/IRIS spectra (reanalyzed here), we find limited inter-annual variations. A return to the 1980 stratospheric temperatures and abundances is generally achieved from 50°N to 50°S, indicative of the solar radiation being the dominating energy source at 10 AU, as for the Earth, as predicted by general circulation and photochemical models. Exceptions concern the most complex hydrocarbons (C_4H_2 and C_3H_4). We also consider data from ground-based and Earth-orbiting observatories (such as from the *Infrared Space Observatory*, revisited here) and discuss possible atmospheric composition trends during a Titanian year.

Key words: molecular processes – planets and satellites: atmospheres – planets and satellites: composition – planets and satellites: individual (Titan) – radiation mechanisms: thermal

1. INTRODUCTION

Mid-2010 *Cassini* observations marked one Titanian year since the first extended space exploration of the satellite by *Voyager 1* (*V1*) during the 1980 November 12 flyby. Titan, Saturn's largest moon, follows its planet on its course around the Sun on an inclined orbit (26.7), which gives rise to seasons, similarly to Earth. The *Cassini* mission had performed 68 Titan flybys by 2010 May (see Tables 1–4 in Bampasidis et al. 2012) when the 9° solar longitude (Ls), was almost exactly the same as at the time of the *V1* flyby (just after spring equinox in the northern hemisphere). Since then, and until the end of 2012, more mid-infrared nadir spectra of Titan were acquired, which we analyze here. These data allow us to probe Saturn's and, especially in what concerns us here, Titan's stratosphere (i.e., altitudes between ∼100 and 400 km above the surface), where neutral gaseous species include hydrocarbons, nitriles, and oxygen compounds.

Stratospheric temperatures and the trace gaseous content, as well as the associated vertical and meridional (latitudinal) distributions, have been reported both from *Voyager* and *Cassini* data over elapsed the time period. Such investigations were first performed on the *V1* Infrared Spectrometer (IRIS) data (e.g., Coustenis & Bézard 1995; Coustenis et al. 1991, and references therein) and between the two Titan *V1* and *V2* thermal infrared datasets (Letourneur & Coustenis 1993) just months apart (the results were quite similar, within the error bars). Since then, several investigators have evaluated the thermal and chemical structure of Titan during the *Cassini* mission (e.g., Achterberg et al. 2008, 2011; Coustenis et al. 2007, 2008, 2010; Vinatier et al. 2007, 2010a, 2010b; Teanby et al. 2008, 2009, 2012; Nixon et al. 2008a, 2008b, 2009, 2013, Cottini et al. 2012). In addition, seasonal variations and trends during the *Cassini* mission were reported (e.g., Teanby et al. 2008, 2009, 2010, 2012; Jennings et al. 2012; Bampasidis et al. 2012). The work we present here has a two-fold aim.

1. On the one hand, we search for seasonal variations within the thermal and chemical structure of Titan's stratosphere during the *Cassini* mission, up to recent observations (end of 2012), covering the northern spring equinox and the beginning of the winter in the southern hemisphere.
2. On the other hand, we search for variations in the temperature and composition of Titan's stratosphere after one Titanian year comparing *V1*/IRIS 1980 and *Cassini*/Composite Infrared Spectrometer (CIRS) 2010 data.

2. OBSERVATIONS

IRIS, a Michelson interferometer that covered the 180–1500 cm^{-1} range (Hanel et al. 1980; Flasar et al. 2004),

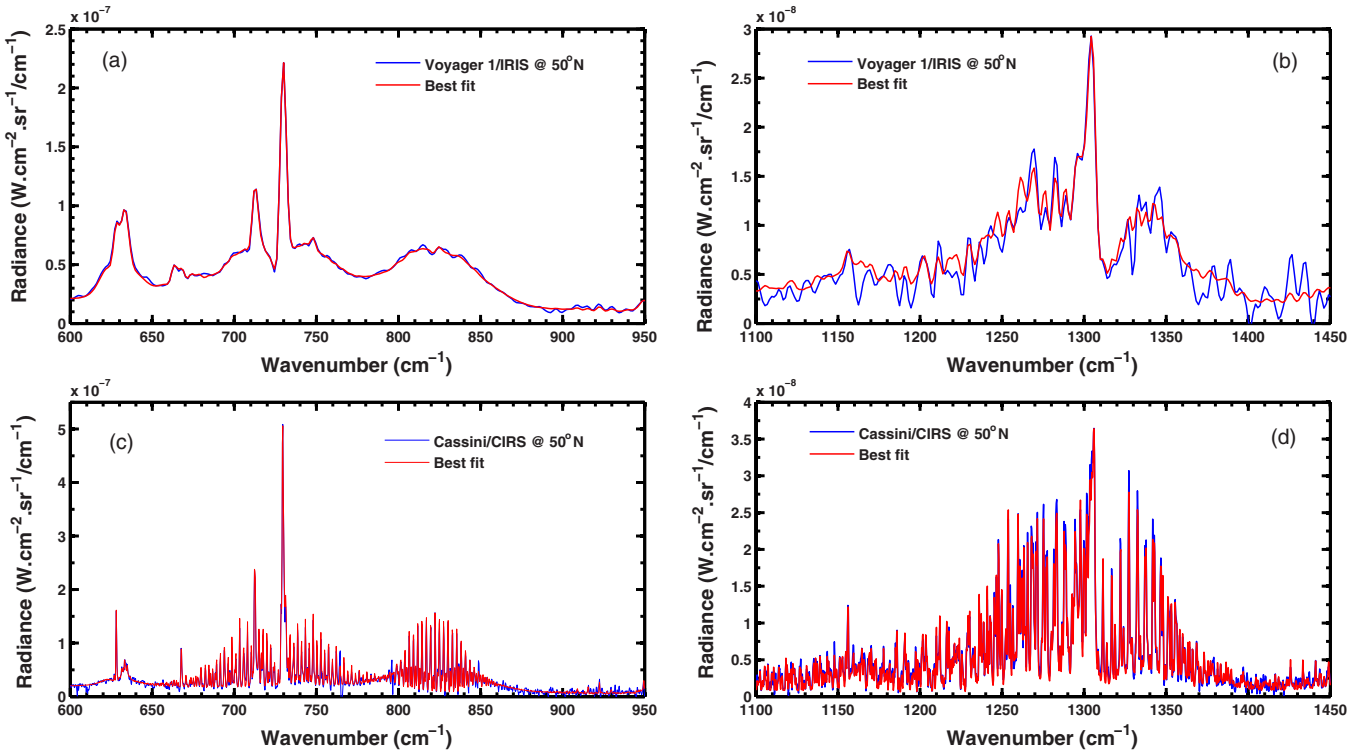

Figure 1. Upper panel: fit of the *V1*/IRIS 1980 November data of Titan taken at 50°N, with the updated code and spectroscopic parameters. The spectral resolution is 4.8 cm^{-1}. The improved fit in the region 670–700 cm^{-1}, with respect to the Coustenis & Bézard (1995) publication, is due to the inclusion of the C_2HD and C_6H_6 bands that were not identified at that time. Lower panel: fit of the 0.5 cm^{-1} resolution CIRS spectrum taken in 2010 January. Left: FP3 region; right: FP4 region.

acquired about 300 usable spectra with a resolution of 4.3 cm^{-1} during the 1980 Titan flyby. Its heir, CIRS, acquired a large number of spectra during the *Cassini* Titan flybys (about 90 by the end of 2012) in the thermal infrared range from 600 to 1430 cm^{-1} (focal plane 3 (FP3; 600–1100 cm^{-1}) and focal plane 4 (FP4; 1100–1430 cm^{-1}) in nadir and limb geometry conditions at high, medium, and low spectral resolutions (0.53, 2.54, and 15 cm^{-1} respectively; Flasar et al. 2005). The CIRS data represent a significant improvement in the number of spectra, spatial coverage, data quality, and spectral resolution (by about an order of magnitude; see Figure 1).

We analyze several averages of CIRS nadir-viewing FP3 and FP4 spectra at medium and high resolution during the *Cassini* mission from July 2004 until 2013, complementing our previous analysis, which stopped in 2010 at flyby T72 (Bampasidis et al. 2012), by including data from 2011 and 2012 *Cassini*/CIRS spectra at 50°N, 50°S, and near the equator. In particular, we have added one selection for 50°N recorded in 2012 September (T86 flyby) with 761 spectra (signal to noise (S/N) = 35.5 and 1.24 airmass) in FP3 and 831 spectra (S/N = 57.6 and 1.28 airmass) in the associated FP4. Similarly, for 50°S, a selection from 2012 September contains 777 spectra (S/N = 22.5 and 1.34 airmass) in FP3 and 612 spectra (S/N = 30.4 and 1.27 airmass) in FP4. At the equatorial latitudes, we have included three more selections recorded in 2012 January, February, and May during the T81, T82, and T83 *Cassini* flybys, respectively, with 1431, 1147, and 617 spectra for each FP3 (S/N: 57.7, 53.3, and 34.5; airmass: 1.19, 1.01, and 1.01, respectively). In the FP4 region, we have 1469, 1131, and 551 spectra for each flyby with a S/N of 129.5, 116.5, and 79.9 and 1.10, 1.11, and 1.01 airmasses, respectively. We note that the viewing conditions (airmass in particular) are very similar for this additional dataset in 2012.

We have also compiled a listing of stratospheric-pertaining, ground-based and *Infrared Space Observatory* (*ISO*; Coustenis et al. 2003) abundance inferences (Table 1). These values are not disk resolved and sometimes refer to different levels in the atmosphere of Titan, so direct comparisons are difficult with the space data, all the more so since the error bars are not firmly defined in most of the ground-based studies. Hereafter, we mainly focus on comparisons between CIRS and IRIS, as these space datasets are the most directly comparable.

3. ANALYSIS

In this work, we use *Cassini*/CIRS data to extend the 2006–2010 study of Bampasidis et al. (2012) until the end of 2012. We combine this with a reanalysis of the *Voyager* data and *ISO* datasets in order to define the neutral chemistry and atmospheric evolution on Titan on timescales longer than a Titanian year. We focus on latitudes from 50°S to 50°N, as these regions have the most complete temporal coverage.

We use our radiative transfer code ARTT (Coustenis et al. 2010; Bampasidis et al. 2012), which includes all currently detected gases in Titan's stratosphere via updated spectroscopic parameters for the main species (CO_2, HCN, C_2H_2, C_2H_6, C_3H_4, C_4H_2, C_3H_8, C_2H_4, HC_3N, and C_6H_6,) and their isotopologues (such as CH_3D, C_2HD, and the ^{13}C or ^{15}N isotopes of C_2H_2, CH_4, HCN, etc.), as available (Coustenis et al. 2003, 2008; Jennings et al. 2008; Nixon et al. 2008a, 2008b, 2009; Rothman et al. 2009; Jacquinet-Husson et al. 2011). The thermal structure is derived using an a priori approach described in Achterberg et al. (2008, 2011) and applied to the *Cassini*/CIRS and *V1*/IRIS data by fitting the ν_4 methane band at 1305 cm^{-1} (Figure 1). The altitude/pressure ranges probed by the temperature profiles depend on the latitude, but are in general between 0.1 and

Table 1
Ground-based and Earth-bound Observations of Titan's Stratospheric Composition

Species	Observ. Date	Ls	Abundance	Altitude (km)	Latitude	Observatory/Instrument	Reference	Resolving Power	Range (cm^{-1})
C_2H_2	1997 January 10	194	$4.92 \pm 0.43 \times 10^{-6}$	Stratosphere	Disk average	*ISO*/SWS	Coustenis et al. (2003)	1650–2000	330–1420
	2001 November 21	257	$7.00 \pm 4.50 \times 10^{-6}$ $5.60 \pm 3.30 \times 10^{-6}$ $4.00 \pm 2.30 \times 10^{-6}$	300 200 100	Disk average	KECK 2/NIRSPEC	Kim et al. (2005)	2.5×10^4	3225–3472
C_2H_4	1974 April to 1975 April	282–295	$1.10 \pm 0.90 \times 10^{-7}$	Stratosphere	Disk average	KPNO?	Gillett (1975) & Orton (1992)	2.0×10^{-2}	Near-IR
	1997 January 10	194	$8.48 \pm 1.00 \times 10^{-8}$	Stratosphere	Disk average	*ISO*/SWS	Coustenis et al. (2003)	1650–2000	330–1420
C_4H_2	1997 January 10	194	$1.67 \pm 0.42 \times 10^{-9}$	Stratosphere	Disk average	*ISO*/SWS	Coustenis et al. (2003)	1650–2000	330–1420
	2001 November 21	257	$<1.00 \times 10^{-7}$	Stratosphere	Disk average	KECK 2/NIRSPEC	Kim et al. (2005)	2.5×10^4	3225–3472
C_2H_6	1974 April to 1975 April	282–295	$1.00 \pm 0.30 \times 10^{-5}$	Stratosphere	Disk average	KPNO/?	Gillett (1975) & Orton (1992)	2.0×10^{-2}	Near-IR
	1993 August	153	$1.96 \pm 2.42 \times 10^{-5}$ $5.80 \pm 3.30 \times 10^{-6}$	Stratosphere Stratosphere	Center West	IRTF/IRHS	Livengood et al. (2002)	1.0×10^6	841–851
	1995 October	179	$9.40 \pm 9.40 \times 10^{-6}$	120–300	Disk average	IRTF/IRHS	Kostiuk et al. (1997)	1.0×10^6	841–851
	1995 October	179	$1.17 \pm 0.44 \times 10^{-5}$ $1.36 \pm 0.71 \times 10^{-5}$	Stratosphere Stratosphere	East West	IRTF/IRHS	Livengood et al. (2002)	1.0×10^6	841–851
	1996 September	190	$1.60 \pm 0.77 \times 10^{-5}$ $5.20 \pm 5.90 \times 10^{-6}$	Stratosphere Stratosphere	East West	IRTF/IRHS	Livengood et al. (2002)	1.0×10^6	841–851
	1993 August to 1996 September	153–190	$8.80 \pm 2.20 \times 10^{-6}$	Stratosphere	Disk average	IRTF/IRHS	Livengood et al. (2002)	1.0×10^6	841–851
	1997 January 10	194	$1.12 \pm 0.45 \times 10^{-5}$	Stratosphere	Disk average	*ISO*/SWS	Coustenis et al. (2003)	1650–2000	330–1420
	2003 December 18	286	$3.00 \pm 1.50 \times 10^{-6}$ $9.00 \pm 5.00 \times 10^{-6}$ $8.00 \pm 3.00 \times 10^{-6}$	Stratosphere Stratosphere 130–300	15N–40S West 5N–50S East Simultaneously east and west	Subaru/HIPWAC	Kostiuk et al. (2005)	$1–25 \times 10^6$	851
	1993 August to 2003 December	153–286	$8.60 \pm 3.00 \times 10^{-6}$	100–300 km	Disk average	IRTF/IRHS & Subaru/HIPWAC	Kostiuk et al. (2010)	1.0×10^6	851
	2005 January 15	300	$9.30 \pm 7.30 \times 10^{-6}$ $8.20 \pm 2.10 \times 10^{-6}$ $9.70 \pm 4.90 \times 10^{-6}$	250–316	Disk center	Subaru/HIPWAC	Livengood et al. (2006)	$1–25 \times 10^6$	851
C_3H_8	1997 January 10	194	$1.67 \pm 0.83 \times 10^{-7}$	Stratosphere	Disk average	*ISO*/SWS	Coustenis et al. (2003)	1850	330–1420
	2002 December 14	272	$6.20 \pm 1.20 \times 10^{-7}$	90–250	Disk average	IRTF/TEXES	Roe et al. (2003)	1.0×10^5	748

Table 1
(Continued)

Species	Observ. Date	Ls	Abundance	Altitude (km)	Latitude	Observatory/Instrument	Reference	Resolving Power	Range (cm^{-1})
	1986 September 8 1987 May 6	76–84	$7.50 \pm 0.80 \times 10^{-8}$ $3.30 \pm 0.90 \times 10^{-7}$ $6.20 \pm 2.10 \times 10^{-7}$ $5.20 \pm 6.60 \times 10^{-6}$	100 170 200 300	Disk average	IRAM	Tanguy et al. (1990)	78 kHz & 1MHz	2.95
	1995 May 22	174	$5.00 \pm 1.10 \times 10^{-8}$ $1.50 \pm 0.50 \times 10^{-7}$ $3.50 \pm 1.10 \times 10^{-7}$	100 170 200	Disk average	IRAM	Hidayat et al. (1997)	78 kHz & 1MHz	2950
	1997 January 10	194	$2.42 \pm 0.40 \times 10^{-7}$	Stratosphere	Disk average	*ISO*/SWS	Coustenis et al. (2003)	1850	330–1420
HCN	1996 April and 1999 December	200 and 232	$4.00 \pm 2.00 \times 10^{-8}$ $2.10 \pm 0.80 \times 10^{-7}$ $4.50 \pm 1.50 \times 10^{-7}$ $5.20 \pm 1.60 \times 10^{-7}$ $5.80 \pm 2.00 \times 10^{-7}$ $6.60 \pm 2.00 \times 10^{-7}$ $7.50 \pm 2.50 \times 10^{-7}$ $8.00 \pm 2.50 \times 10^{-7}$	100 170 200 250 300 350 400 450	Disk average	IRAM	Marten et al. (2002)	78 kHz & 1MHz	2960 & 8620
	2001 November 21	257	$1.00 \pm 0.20 \times 10^{-7}$ $4.10 \pm 2.00 \times 10^{-7}$ $1.00 \pm 0.25 \times 10^{-6}$ $5.00 \pm 2.00 \times 10^{-6}$	200 300 400 500	Disk average	KECK 2/NIRSPEC	Kim et al. (2005)	2.5×10^4	3225–3472
	2004 February 1	288	$3.00 \pm 1.00 \times 10^{-7}$ $4.00 \pm 2.00 \times 10^{-7}$ $5.00 \pm 5.00 \times 10^{-6}$	83 200 300	Disk average	SMA	Gurwell (2004)		11.5
	2010 July	11	$1.5\ 10^{-7}$	125	Disk average	*Herschel*/SPIRE	Courtin et al. (2011)	~375	20–52
C_3H_4	1997 January 10	194	$1.19 \pm 0.40 \times 10^{-8}$	Stratosphere	Disk average	*ISO*/SWS	Coustenis et al. (2003)	1650–2000	330–1420
CO_2	1997 January 10	194	$1.82 \pm 0.18 \times 10^{-8}$	Stratosphere	Disk average	*ISO*/SWS	Coustenis et al. (2003)	1650–2000	330–1420

Notes. These data provide information about the atmospheric composition of Titan during the interval between the *Voyager* and *Cassini*/Huygens missions, but are not directly comparable with the conclusions derived from spatially resolved interplanetary spacecraft observations. Details of the observatory and instrument are provided in the corresponding references.

Table 2
New values of *V1*/IRIS 1980 abundance retrievals at 50°S, the equator, and 50°N with 3σ error bars including both systematic and random uncertainties

Molecule	50°S	7°N	50°N	*ISO* Disk Average
C_2H_2	$2.25 \pm 0.45 \times 10^{-6}$	$2.62 \pm 0.4 \times 10^{-6}$	$3.35 \pm 1.0 \times 10^{-6}$	$4.95 \pm 0.5 \times 10^{-6}$
C_2H_4	$1.14 \pm 0.45 \times 10^{-7}$	$1.13 \pm 0.3 \times 10^{-7}$	$2.55 \pm 1.22 \times 10^{-7}$	$9.33 \pm 0.4 \times 10^{-8}$
C_2H_6	$9.50 \pm 1.85 \times 10^{-6}$	$1.01 \pm 0.15 \times 10^{-5}$	$1.35 \pm 0.34 \times 10^{-5}$	$1.32 \pm 0.5 \times 10^{-5}$
C_3H_4	$5.60 \pm 1.75 \times 10^{-9}$	$7.80 \pm 1.6 \times 10^{-9}$	$3.10 \pm 0.93 \times 10^{-8}$	$1.44 \pm 0.4 \times 10^{-8}$
C_3H_8	$1.40 \pm 0.6 \times 10^{-6}$	$1.60 \pm 2.2 \times 10^{-6}$	$2.10 \pm 1.0 \times 10^{-6}$	$4.76 \pm 0.8 \times 10^{-7}$
C_4H_2	$1.30 \pm 0.35 \times 10^{-9}$	$1.57 \pm 0.4 \times 10^{-9}$	$1.10 \pm 0.4 \times 10^{-8}$	$2.09 \pm 0. \times 10^{-9}$
HCN	$7.50 \pm 2.2 \times 10^{-8}$	$2.03 \pm 0.4 \times 10^{-7}$	$7.00 \pm 2.7 \times 10^{-7}$	$2.97 \pm 0.4 \times 10^{-7}$
CO_2	$1.55 \pm 0.27 \times 10^{-8}$	$1.50 \pm 0.2 \times 10^{-8}$	$1.00 \pm 0.3 \times 10^{-8}$	$2.05 \pm 0.2 \times 10^{-8}$

Notes. The *ISO* values were also re-calculated with a temperature profile matching the emission observed in the CH_4 ν_4 band at 1304 cm^{-1} and the new spectroscopic data available for some molecules. The corresponding altitudes are the same as in Coustenis et al. (2003). The re-analysis of the *V1*/IRIS data allowed us to detect in them for the first time C_6H_6, HC_3N, and C_2HD (see the fit in Figure 1), albeit given the low spectral resolution of the *Voyager* spectra, we were unable to derive accurate mixing ratios for these molecules and therefore they are excluded from this paper. The same pertains to C_3H_8 and C_2H_4, which have large uncertainties (see the text). The *V1*/IRIS abundances are compared with the CIRS 2010 mixing ratios in Figure 3.

20 mbar. We then use the temperature profile in our radiative transfer code to derive the chemical composition of the trace gases in the rest of the spectrum (for details, see Coustenis & Bézard 1995; Coustenis et al. 2003, 2010; Bampasidis et al. 2012; the calculated contribution functions peak around 2–4 mbar for C_2H_2 and 5–7 mbar for the other molecules, depending on the latitude and the molecule).

We apply this method to different latitudes from 50°N to 50°N for CIRS and IRIS. The mixing ratios are assumed to be vertically constant profiles above the condensation level and the altitudes probed for all space data correspond in general essentially to the altitude range of 80–300 km (0.1–20 mbar; see Coustenis et al. 2010 and Bampasidis et al. 2012 for more details). The C_2H_2 vertical profile is rather constant in the lower stratosphere, as determined by a combination of limb and nadir CIRS data near the equator and at northern latitudes (e.g., Vinatier et al. 2007), so that our acetylene non-varying vertical profile is not incompatible with the true situation. However, when the C_2H_2 band is not properly fit in the entire spectral range (over 700–750 cm^{-1}) with such a profile and solely one mixing ratio above the condensation level, we determine the abundance that best fits the *Q*-branch and then the one that allows us to satisfy the emission in the wings, minimizing the residuals. The two mixing ratios only differ slightly (see Coustenis et al. 2010). We then derive the other abundances from the rest of the spectrum. When this is the case, we give an averaged mixing ratio in the results (for details, see Coustenis & Bézard 1995; Coustenis et al. 2010). The contribution functions for these molecules remain within the ranges determined in these previous papers (generally around 2–4 mbar for C_2H_2 and in the 5–10 mbar region for the other trace gases; for more details, see Figure 5 of Coustenis et al. 2010).

Our comparison with *V1*/IRIS data is restrained to those molecules with strong enough emission bands to be unambiguously detected also in the *Voyager* spectra with high enough S/N and sufficient accuracy. These molecules are: CO_2, HCN, C_2H_2, C_2H_6, C_3H_4, and C_4H_2. In this analysis, we do not include the results we infer for C_3H_8 and C_2H_4, which are difficult to exploit in the *V1*/IRIS spectra since they have weak and/or blended bands and suffer from higher uncertainty than the other molecules in the CIRS data.

Table 2 shows the re-analyses of the *V1*/IRIS data (updating Coustenis & Bézard 1995) and of the *ISO* Short Wavelength Spectrometer (SWS) disk-averaged spectrum (updating Coustenis et al. 2003) using the same model as for the CIRS data. The differences between our work and previous publications are minor, except for the molecules that benefited from significantly improved spectroscopic parameters.

4. RESULTS OF THE STRATOSPHERIC STRUCTURE DURING ONE TITANIAN YEAR

The best fits obtained for the *V1*/IRIS 1980 and the 2010 January *Cassini*/CIRS 50°N selections are shown in Figure 1.

4.1. Inter-annual Temperature Variations

We compare the new temperature profiles inferred for the *Voyager* selections with the ones found for 2010 from CIRS data at 50°N, the equator, and 50°S (Figure 2). We also overplot on the figure the temperature profile that corresponds to the disk-average *ISO* observations of 1997, which pertain most closely to conditions at mid-latitudes.

In the southern hemisphere, the 1980 and 2010 temperature profiles are quite similar, with very small differences of less than 5 K and more typically 2–3 K between 0.1 (250 km) and 10 mbar (100 km) in the region probed by our data. Above the 0.1 mbar pressure level, the temperature appears to be cooling, e.g., by as much as 15 K at 0.01 mbar (400 km) from 2005 to 2010 (Achterberg et al. 2011) and although the inferences at high altitudes suffer from high uncertainties when derived from nadir data, the limb findings (Vinatier et al. 2007, 2010b; Teanby et al. 2012) confirm these results. The reader is referred to such limb-data analyses for more details on the temperatures at higher altitudes. The revised *Voyager* temperature profiles are then consistent with the CIRS 2010 ones in the lower latitudes and no significant variations are detected.

Similarly, no significant change was found in the equatorial mid-stratospheric temperatures, with the 1980 and the 2010 temperature profiles always within 5–6 K of each other up to the 0.1 mbar level, although again it appears that a cooler equatorial mesosphere is observed after one Titanian year as in the south. We note that the temperature profile corresponding to the *ISO* 1997 data follows very closely the CIRS 2010 profile throughout the equatorial stratosphere. All in all, the average vertical stratospheric temperature profiles from 50°S to the equator appear quite similar to each other at all times. The 50°S temperatures are about 3–6 K cooler than the equatorial ones for CIRS (see, e.g., Bampasidis et al. 2012 for more

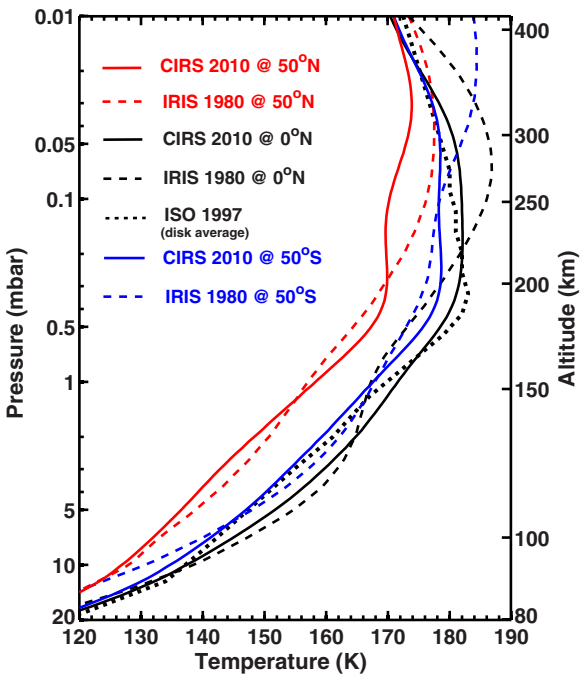

Figure 2. Retrieved thermal profiles from CIRS and *V1*/IRIS data (in the solid and dashed lines, respectively) at 50°S, 50°N, and equator for the 2010 nadir data and the IRIS 1980 data. The CIRS temperature profiles correspond to 2010 April, July, and January at 50°S, the equator, and 51°N, respectively. The temperature profile corresponding to the *ISO* disk-averaged SWS data of 1997 is also shown in dotted black lines. The pressure/altitude ranges probed by these profiles vary with latitude, but are generally in the 0.1–20 mbar region (see the text). The uncertainty is about 1 K at 1 mbar and 5 K at 5 mbar for the CIRS profiles and about 1 K more at each level for the IRIS profiles due to the higher noise. For *ISO*, the error bars are about 2 K at pressures lower than 1 mbar and are at most 5 K at higher ones (altitudes lower than 200 km).

precise information on the thermal evolution during the *Cassini* mission).

At northern latitudes, temporal variations were reported during the *Cassini* mission (2004–2012), with the shape of the thermal structure changing toward a more vertically homogeneous profile in the past 4 yr and not showing the marked stratopause observed earlier, among other changes (Achterberg et al. 2011; Bampasidis et al. 2012; Teanby et al. 2010, 2012). However, when we compare the 1980 and the 2010 stratospheric profiles at 50°N, we find the *V1* profile to be quite compatible with the CIRS one, equivalent to within 3–4 K up to the 0.2 mbar (220 km) level. Thus, in the stratosphere, the thermal structure has returned to the *V1* shape after a Titanian year (Figure 2).

4.2. Chemical Composition Variations

With the temperature profiles determined as indicated above, we infer the chemical composition for Titan's stratosphere from CIRS, IRIS, and *ISO* spectra. The new and more accurate chemical composition inferred at the time of the *V1* encounter (1980 November 12) is given in Table 2 for the latitudes of interest here. The revised abundances for the *ISO*/SWS data of 1997 are also listed in that table.

The CIRS composition determinations from high-resolution (0.5 cm^{-1}) spectra with respect to the *V1*/IRIS inferred values are shown in Figure 3 for C_2H_2, C_2H_6, C_3H_4, C_4H_2, HCN, and CO_2 at 50°S, the equator, and 50°N. Since the model parameters for all these calculations are the same, we only consider the relative uncertainties that are due to the data noise and calibration uncertainties (since a large number of spectra are summed, this cause for error is small), as well as the temperature profile inferences (see Coustenis et al. 2010 and Bampasidis et al. 2012 for details). In Figure 3, we display only these relative error bars for all the molecules so that we can derive the variations with time within the *Cassini* mission period for each species. The re-estimated abundances for *V1*/IRIS are also indicated in Figure 3 for 2010 May, when such a comparison is meaningful, and the uncertainty due to the *V1*/IRIS random errors (noise, calibration, temperature profile determination, and fit of the continuum) is then taken into account. We note that the error due to the use of a constant-with-height versus an altitude-dependent profile even at different viewing geometries is less than 7% and therefore small with respect to some of the other uncertainties described above, but we take it into account when comparing data at significantly different airmasses. When the *V1*/IRIS results from a Titanian year ago are compared with the CIRS results derived at the mid-2010 date (Figure 3), we see a hint of the potential inter-annual variations after 30 Earth years for 50°S, the equator, and 50°N.

Hereafter, we discuss for each molecule: (1) the trend during the *Cassini* mission until end of 2012 and (2) the comparison between the CIRS inferences around mid-2010 with the abundances found a Titanian year ago.

4.2.1. Seasonal Evolution of the Stratospheric Composition

Figure 3 shows the composition of Titan's stratosphere during the *Cassini* mission, from 2006 until 2013, at three latitudes.

Starting with the lower latitudes (50°S), we find that during the *Cassini* mission, the stratospheric abundances are lower than at mid or northern latitudes. Furthermore, the CIRS high-resolution data indicate that, within the measurement uncertainties, C_2H_2, C_2H_6, and CO_2 can be considered to be unvarying up to 2013 (Figures 3(a), (e), and (f)), as indicated also in Bampasidis et al. (2012) for up to 2011, while HCN, C_4H_2, and C_3H_4 show some excursions in the last 2 yr (Figures 3(b), (c), and (d)). Indeed, we note that the results from the analysis of the 2012 September selection indicate that the latter gases exhibit a significant increase in their abundances, in agreement with the expected seasonal reversal in Titan's stratospheric composition for some of the most short-lived gases and the haze (see also Teanby et al. 2012; Jennings et al. 2012, and references therein for this phenomenon). CO_2 also exhibits a trend for an increase at 50°S but this trend is also seen at 50°N and the error bars are too large enough to allow for a definitive inference.

In the equatorial region, where we have more spectra in the recent years, the mixing ratios are in general higher than at 50°S, especially for HCN (Figure 3(b)). We find the stratospheric composition evolution to be rather uneventful and regular for all molecules during the mission, with perhaps a trend for a slight decrease in 2012 (except for C_3H_4, which remains constant) that needs to be confirmed.

At 50°N, as noted also in Bampasidis et al. (2012), we find that, with the possible exception of C_2H_6, CO_2, and C_3H_4, all the molecules show significant variations with time during the *Cassini* mission. Thus, while from 2007 to mid-2008 the gas mixing ratios are constant to within 30%, we detect a general trend for a pronounced increase from mid-2008 to mid-2009 with a maximum (by factors of 2–3) for almost all molecules in 2009 April-May (the time closest to Titan's northern spring equinox is 2009 August). This is followed by a strong decrease, which reduces the 2010 concentrations to the values of the period preceding the increase (Figure 3) and is confirmed in the 2012 September data.

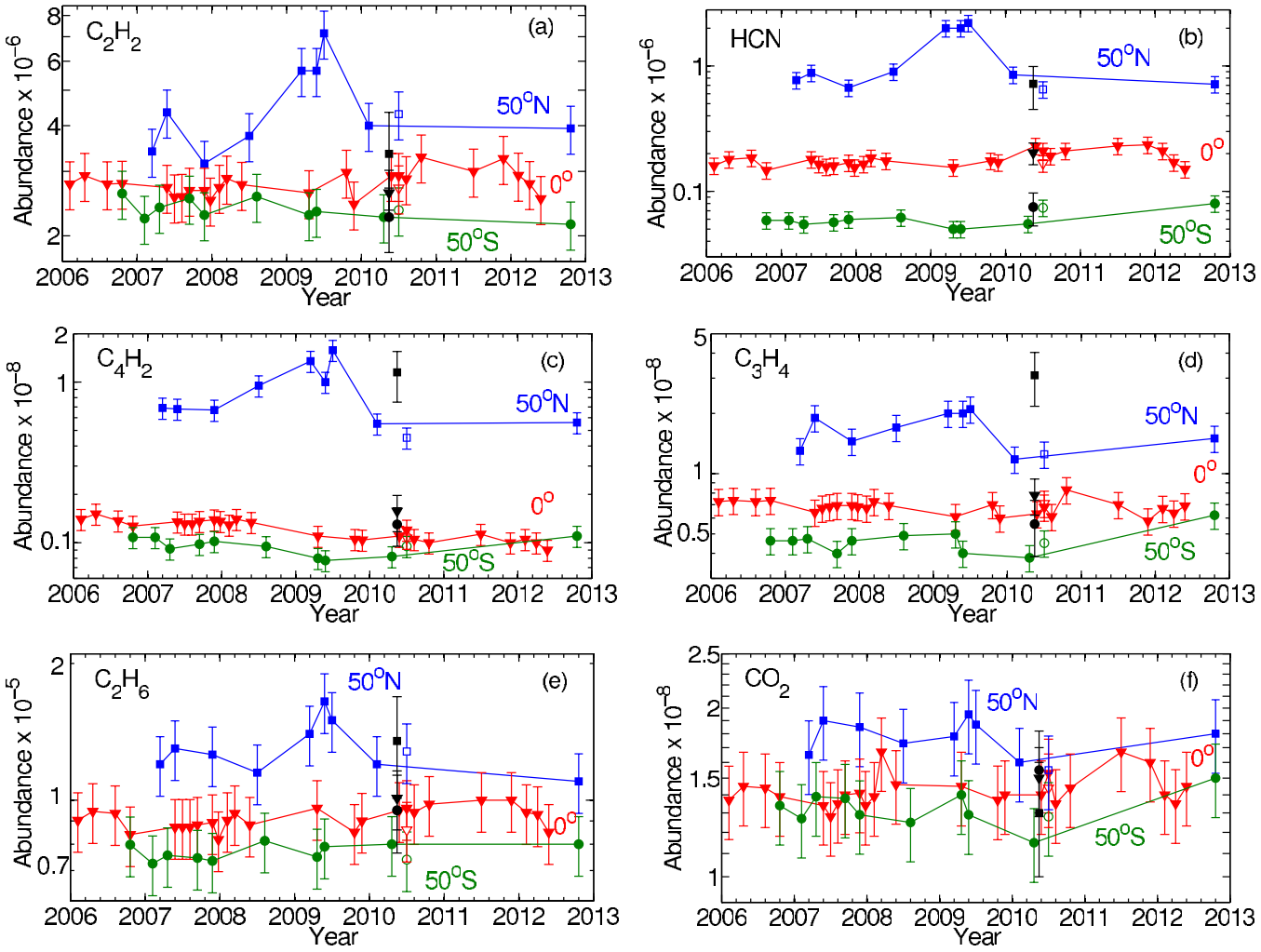

Figure 3. Variations of the abundances of gases in Titan's stratosphere during the *Cassini* mission at 50°S (solid green circles and lines), the equator (red full triangles and lines), and 50°N (solid blue squares and lines) inferred from high-resolution nadir data for: (a) C_2H_2, (b) HCN, (c) C_4H_2, (d) C_3H_4, and (e) C_2H_6 and CO_2. The open symbols correspond to mixing ratio inferences from medium-resolution (2.5 cm^{-1}) data that we have in 2010. The black symbols and vertical lines correspond to the recalculated *V1*/IRIS abundances and error bars.

4.2.2. Inter-annual Compositional Variations

We then compare high-resolution CIRS mid-2010 abundances with the retrievals of the *V1*/IRIS (1980) re-analyses by computing the abundances for certain molecules. For comparison's sake with the *V1*/IRIS data (resolution of 4.3 cm^{-1}), we have also included some abundance retrievals from medium-resolution (2.5 cm^{-1}) CIRS spectra for 2010, when available. In general, the high- and the medium-resolution abundances are in agreement within the error bars, although slight differences can exist of up to 10%–15% (Figure 3), which can be the result of a small difference in the altitudes probed or the time of the observations The *V1*/IRIS results are plotted in black symbols in Figure 3.

All the molecules show compatible results between the *V1*/IRIS and the *Cassini*/CIRS mixing ratio inferences in the equatorial region (Figure 3, triangles) within the error bars, for all spectral resolutions. We have thus returned in 2010 to the same stratospheric composition as a Titanian year ago.

At 50°S, the 2010 April high-resolution (Figure 3, full circles) and May-June medium-resolution (Figure 3, open circles) spectra yield quite compatible results. All gaseous abundances from the 2010 CIRS datasets (when both the higher and medium resolution measurements are taken into account) are compatible with the values observed in 1980 by *V1* within the error bars for the southern latitudes (Figure 3). CO_2, C_4H_2, and C_3H_4 appear to have lower abundances in 2010, but the uncertainties on these molecules are larger due to their proximity with other species. However, we note that when the medium-resolution results are also taken into account, there is no real indication for a departure from a similar composition anywhere so far. CO_2 shows a particular behavior (Figure 3(f)), in that the *V1*/IRIS data show a decrease in abundance from south to north (as noted in Coustenis & Bézard 1995), which we do not find in the *Cassini*/CIRS inferences. When all the uncertainties are taken into account, we cannot infer a different CO_2 composition after a Titanian year.

In general, at 50°N (Figure 3, squares open or filled), we find in 2010 a return to the *V1*/IRIS values within the 35% uncertainty level for all molecules except the two complex hydrocarbons C_4H_2 and C_3H_4, which stay well below the 1980 abundances by about 50%–55% (Figures 3(c) and (d)). Again, the 2010 May 50°N CIRS nadir data at 2.5 cm^{-1} are close to the high-resolution values (differing by no more than ±15%).

We also considered ground-based and disk-averaged *ISO* data obtained before *Cassini* or more recently with *Herschel* (see Table 1). These data are limited in general to a few molecules such as C_2H_2, C_2H_6, and HCN (Table 1) and the snapshots

we have between 1980 and the *Cassini* mission show no large departures in abundance from one season to another or within a Titanian year for these few molecules, as far as we can tell from the analyses published over the years. The data from *ISO*/SWS taken in 1997 toward the northern fall equinox (NFE, occurring in 1995) concern more molecules (CO_2, C_3H_4, and C_4H_2, in addition to the previous ones) and seem to yield somewhat higher values for the species discussed here, such as HCN and C_2H_2. One of the rare models dealing with long-term variations in Titan's atmosphere (over a Titanian year starting in 2000) was produced by Hourdin et al. (2004). Their Figure 9 shows that soon after NFE, in the 80–240 km altitude range, the high-latitude HCN concentration grows very fast under the effect of downward advection, as do the latitudinal contrasts with low latitudes, reaching a maximum. It follows that the *ISO* disk-averaged data, which include some of the polar enhancement in gaseous components observed at NFE, may indeed exhibit higher values than any disk-resolved, space-equivalent data. However, it is very difficult to conclude that the *ISO* values are indeed higher than the *V1*/IRIS or the CIRS ones, given the impossibility of properly assessing and comparing ground-based or Earth-bound observations with space in situ ones, given the differences in spectral resolution, altitudes and regions probed, modeling parameters by different investigators, etc. We note, however, that the HCN stratospheric vertical profile obtained by *Herschel*/SPIRE recently (Courtin et al. 2011) for 2010 July is in good agreement with our findings at around 5 mbar (125 km in altitude) for equatorial latitudes ($\sim 1.5 \times 10^{-7}$; Figure 3 in Bampasidis et al. 2012; Figure 5(b) and Table 2 of Coustenis et al. 2010), given that we only consider constant vertical profiles.

We also note that the results of a recent analysis of CIRS limb data (Vinatier et al. 2012) at 50°S, 1°N, and 51°N taken in 2010 June, but covering higher altitudes (up to 500 km) and the simple vertical distributions of some hydrocarbons and nitriles retrieved from scarce horizontal viewing *V1*/IRIS data (Coustenis et al. 1991) are consistent with the general trend showing the nitriles increasing with altitude faster than the hydrocarbons. But again, the comparison cannot be pushed too far given the differences in vertical resolution, modeling, gaseous distributions, thermal structure, etc.

5. DISCUSSION

The fulfillment of one Titanian year of observations provides us for the first time with the opportunity to evaluate the relative role of different physical processes in the long-term evolution of this complex environment. By comparing *V1* (1980), *ISO* (1997), and *Cassini* (2010) data, we find that the temperature structure is quite similar within the error bars (Figure 2). The chemistry also appears to be generally unchanging (*V1*/IRIS data versus *Cassini*/CIRS data are within 25%–35%), with some exceptions among the more complex hydrocarbons such as C_3H_4 and C_4H_2, which are short-lived and low-abundance species in Titan's stratosphere and hence are more prone to inter-annual variations.

The detection of long-term temporal variations of the atmospheric chemical composition and thermal structure informs us of the impact of different processes such as photochemistry and dynamics. The main energy source defining Titan's chemical composition is solar radiation, while energetic particles from Saturn's magnetosphere, as well as Galactic cosmic rays, also contribute significantly. All of these energy sources vary temporally in magnitude during the course of one Titanian year. The return of today's abundances to values close to the ones derived from *Voyager* spectra (at the same season) is an indication that, as for the Earth, solar radiation dominates over other energy sources, even at 10 AU. Nevertheless, the differences observed (lower C_3H_4 and C_4H_2 mixing ratios) and the slightly higher values observed from the ground and from *ISO* near the NFE could suggest that other processes may be at play as well, for example, the variability of the solar insolation itself through the 11 yr solar cycle or complex circulation phenomena. Indeed, and although it may not explain the totality of the variations observed, we note that due to the 11 yr solar cycle, which is related to the oscillation of the Sun's magnetic field, the total solar irradiance is not constant. This variability has a strong spectral dependence that is related to the fact that different energy photons originate from different regions of the solar atmosphere. For wavelengths longer than 260 nm, which originate from the photosphere, the variability is very small, less than 0.1% during the solar cycle (Woods & Rottman 2002). This is the spectral region of the solar irradiance that can be approximated by blackbody emission (although, between 400 and 200 nm, strong absorption lines and absorption-edge effects lead to a deviation from a blackbody curve). Higher energy photons originate from regions extending above the photosphere (the chromosphere, the transition region, and the corona), which are in non-local thermodynamic equilibrium conditions. At these wavelengths, the observed solar irradiance is dominated by the presence of strong emission lines, which are sensitive to the solar magnetic activity. Here, the solar cycle variability increases toward shorter wavelengths. At 200 nm, the variation between the minimum and maximum observed irradiance is about 10%, while at the Lyα line (121.6 nm), the largest observed increase is a factor of about 1.6. For higher energies, the variability is even larger (Woods & Rottman 2002). Therefore, given that the photochemistry in Titan's atmosphere (and also in any other atmosphere) is driven dominantly by Lyα photons and the fact that all observed species are a result of photochemistry, the 11 yr solar cycle can affect the temporal evolution of the observed chemical abundances.

We also note from the variations during the *Cassini* mission found for the gases investigated here that in the South pole some of the short-lived minor species tend to show a strong increase in 2012, in accordance with what is expected from seasonal models of Titan, indicating that a reversal of the north-south asymmetry is ongoing and confirming the trend seen at higher altitudes in CIRS limb data (e.g., Teanby et al. 2012). The seasonal change is found to seriously affect the circulation patterns in Titan's atmosphere. Evidence for the vortex dissipation in the north is found in the temperature decrease (and hence the ending of subsidence) and the decreasing gas enrichment (Bampasidis et al. 2012; Teanby et al. 2012). Conversely, as the southern hemisphere passes into fall, subsidence is now indicated in the south (with rates estimated to about 1–2 mm s^{-1}; Teanby et al. 2012) through the temperature increase since mid-2009 and the chemical composition enhancement since 2011. The circulation now extends to above 500 km in altitude in the south and ample evidence of the expected seasonal reversal of the stratospheric circulation is found with increased northern insolation leading to upwelling at the south pole and consequent (or subsequent) downwelling at the south pole (Teanby et al. 2012). At southern latitudes, above 50°S (as also shown in our work here), we then find an increase in short-lived gas species advected downward in the stratosphere from the higher altitude levels.

The temporal and spatial (due to Titan's inclination) variations in the energy input to Titan's atmosphere is a driver for changes

in the advection patterns, which in turn provide a stronger variability in the latitudinal abundances of photochemical species. Furthermore, both the changes in the energy field and the dynamics affect the production and evolution of aerosols in Titan's atmosphere (Jennings et al. 2012). The abundance peak corresponds to a period during which the observed collapse of the detached aerosol layer (West et al. 2011) suggests that the dynamics went through a rapid transition that should influence the gas distribution and can be tied to the atmospheric circulation reversal predicted by general circulation numerical models (Hourdin et al. 2004; Rannou et al. 2005; Crespin et al. 2008; Lebonnois et al. 2012). At the same time, the variable north/south asymmetry in Titan's albedo and haze content reveals the consequences of seasonal changes in the aerosol properties deeper in the atmosphere (Jennings et al. 2012).

Circulation and photochemical models must satisfy the constraints set by these new results and further observational constraints will come from data acquired during the *Cassini* mission and up until the next summer solstice (2017). We note that we are still lacking disk-resolved data of the atmospheric composition for seasons from summer to winter solstice in the northern hemisphere.

We thank Florence Henry, Marcia Segura, and Nicolas Gorius for help with the data during this project. We are grateful to Pascal Rannou and Sebastien Lebonnois for discussions on general circulation models. The authors acknowledge the support of the ESA/NASA *Cassini* mission funds through the CNES program. A.C. and S.V. received support from the Agence Nationale de la Recherche (ANR project "APOSTIC" #11BS56002, France). N.A.T. received support from the UK Science and Technology Facilities Council and the Leverhulme Trust. Support for G.O. was provided by NASA to the Jet Propulsion Laboratory, California Institute of Technology.

REFERENCES

Achterberg, R. K., Conrath, B. J., Gierasch, P. J., Flasar, F. M., & Nixon, C. A. 2008, Icar, 194, 263
Achterberg, R. K., Gierasch, P. J., Conrath, B. J., Flasar, F. M., & Nixon, C. A. 2011, Icar, 211, 686
Bampasidis, G., Coustenis, A., Achterberg, R. K., et al. 2012, ApJ, 760, 144
Cottini, V., Nixon, C. A., Jennings, D. E., et al. 2012, Icar, 220, 855
Courtin, R., Swinyard, B. M., Moreno, R., et al. 2011, A&A, 536, L2
Coustenis, A., Achterberg, R., Conrath, B., et al. 2007, Icar, 189, 35
Coustenis, A., & Bézard, B. 1995, Icar, 115, 126
Coustenis, A., Bezard, B., Gautier, D., Marten, A., & Samuelson, R. 1991, Icar, 89, 152
Coustenis, A., Jennings, D. E., Jolly, A., et al. 2008, Icar, 197, 539
Coustenis, A., Jennings, D. E., Nixon, C. A., et al. 2010, Icar, 207, 461
Coustenis, A., Salama, A., Schulz, B., et al. 2003, Icar, 161, 383
Crespin, A., Lebonnois, S., Vinatier, S., et al. 2008, Icar, 197, 556
Flasar, F. M., Achterberg, R. K., Conrath, B. J., et al. 2005, Sci, 308, 975
Flasar, F. M., Kunde, V. G., Abbas, M. M., et al. 2004, SSRv, 115, 169
Gillett, F. C. 1975, ApJL, 201, L41
Gurwell, M. A. 2004, ApJL, 616, L7
Hanel, R., Crosby, D., Herath, L., et al. 1980, ApOpt, 19, 1391
Hidayat, T., Marten, A., Bezard, B., et al. 1997, Icar, 126, 170
Hourdin, F., Lebonnois, S., Luz, D., & Rannou, P. 2004, JGR, 109, E12
Jacquinet-Husson, N., Crepeau, L., Armante, R., et al. 2011, JQSRT, 112, 2395
Jennings, D. E., Anderson, C. M., Samuelson, R. E., et al. 2012, ApJL, 761, L15
Jennings, D. E., Nixon, C. A., Jolly, A., et al. 2008, ApJL, 681, L109
Kim, S. J., Geballe, T. R., Noll, K. S., & Courtin, R. 2005, Icar, 173, 522
Kostiuk, T., Fast, K., Livengood, T. A., et al. 1997, P&SS, 45, 931
Kostiuk, T., Hewagama, T., Fast, K. E., et al. 2010, P&SS, 58, 1715
Kostiuk, T., Livengood, T. A., Hewagama, T., et al. 2005, GeoRL, 32, 22205
Lebonnois, S., Burgalat, J., Rannou, P., & Charnay, B. 2012, Icar, 218, 707
Letourneur, B., & Coustenis, A. 1993, P&SS, 41, 593
Livengood, T. A., Hewagama, T., Kostiuk, T., Fast, K. E., & Goldstein, J. J. 2002, Icar, 157, 249
Livengood, T. A., Kostiuk, T., Sonnabend, G., et al. 2006, JGRE, 111, E11
Marten, A., Hidayat, T., Biraud, Y., & Moreno, R. 2002, Icar, 158, 532
Nixon, C. A., Achterberg, R. K., Vinatier, S., et al. 2008a, Icar, 195, 778
Nixon, C. A., Jennings, D. E., Bézard, B., et al. 2008b, ApJL, 681, L101
Nixon, C. A., Jennings, D. E., Bézard, B., et al. 2013, ApJL, 776, L14
Nixon, C. A., Jennings, D. E., Flaud, J.-M., et al. 2009, P&SS, 57, 1573
Orton, G. 1992, in Symposium on Titan (ESA SP-338; Noordwijk: ESA), 81
Rannou, P., Lebonnois, S., Hourdin, F., & Luz, D. 2005, AdSpR, 36, 2194
Roe, H. G., Greathouse, T. K., Richter, M. J., & Lacy, J. H. 2003, ApJL, 597, L65
Rothman, L. S., Gordon, I. E., Barbe, A., et al. 2009, JQSRT, 110, 533
Tanguy, L., Bezard, B., Marten, A., et al. 1990, Icar, 85, 43
Teanby, N. A., Irwin, P. G. J., de Kok, R., et al. 2008, Icar, 193, 595
Teanby, N. A., Irwin, P. G. J., de Kok, R., et al. 2009, RSPTA, 367, 697
Teanby, N. A., Irwin, P. G. J., de Kok, R., & Nixon, C. A. 2010, ApJL, 724, L84
Teanby, N. A., Irwin, P. G. J., Nixon, C. A., et al. 2012, Natur, 491, 732
Vinatier, S., Bézard, B., Anderson, C. M., et al. 2012, in Titan Through Time II Workshop, ed. V. Cottini, C. Nixon, & R. Lorentz, 45
Vinatier, S., Bézard, B., Fouchet, T., et al. 2007, Icar, 188, 120
Vinatier, S., Bézard, B., de Kok, R., et al. 2010a, Icar, 210, 852
Vinatier, S., Bézard, B., Nixon, C. A., et al. 2010b, Icar, 205, 559
West, R. A., Balloch, J., Dumont, P., et al. 2011, GeoRL, 38, L06204
Woods, T. N., & Rottman, G. J. 2002, in Atmospheres in the Solar System: Comparative Aeronomy, ed. M. Mendillo, A. Nagy, & J. H. Waite (Washington, DC: AGU), 221